

## State of the Art: Consensus recommendations on the use of $^{18}\text{F}$ -FDG PET/CT in lung disease

Delphine L. Chen<sup>1</sup>, Safia Ballout<sup>2</sup>, Laigao Chen<sup>3</sup>, Joseph Cheriyan<sup>4,5</sup>, Gourab Choudhury<sup>6</sup>, Ana M. Denis-Bacelar<sup>7</sup>, Elise Emond<sup>8</sup>, Kjell Erlandsson<sup>8</sup>, Marie Fisk<sup>5</sup>, Francesco Fraioli<sup>8</sup>, Ashley M. Groves<sup>8</sup>, Roger N. Gunn<sup>9,10</sup>, Jun Hatazawa<sup>11</sup>, Beverley F. Holman<sup>12</sup>, Brian F. Hutton<sup>8</sup>, Hidehiro Iida<sup>13</sup>, Sarah Lee<sup>14</sup>, William MacNee<sup>6</sup>, Keiko Matsunaga<sup>11</sup>, Divya Mohan<sup>15</sup>, David Parr<sup>16</sup>, Alaleh Rashidnasab<sup>8</sup>, Gaia Rizzo<sup>9,10</sup>, Deepak Subramanian<sup>17</sup>, Ruth Tal-Singer<sup>15</sup>, Kris Thielemans<sup>8</sup>, Nicola Tregay<sup>5</sup>, Edwin J.R. van Beek<sup>6</sup>, Laurence Vass<sup>5</sup>, Marcos F. Vidal Melo<sup>18</sup>, Jeremy W. Wellen<sup>19</sup>, Ian Wilkinson<sup>4,5</sup>, Frederick J. Wilson<sup>20</sup>, Tilo Winkler<sup>18</sup>

<sup>1</sup>*Department of Radiology, University of Washington, Seattle Cancer Care Alliance, Seattle, Washington, USA;*

<sup>2</sup>*School of Physics and Astronomy, University of Leeds, Leeds, United Kingdom;*

<sup>3</sup>*Worldwide Research Development and Medical, Pfizer Inc., Cambridge, Massachusetts, USA;*

<sup>4</sup>*Cambridge University Hospitals NHS Foundation Trust, Cambridge, United Kingdom;*

<sup>5</sup>*Department of Medicine, University of Cambridge, Cambridge, United Kingdom;*

<sup>6</sup>*Edinburgh Imaging, Queen's Medical Research Institute, University of Edinburgh, Edinburgh, United Kingdom;*

<sup>7</sup>*National Physical Laboratory, Teddington, United Kingdom;*

<sup>8</sup>*Institute of Nuclear Medicine, University College London, London, United Kingdom;*

<sup>9</sup>*inviCRO, London, United Kingdom;*

<sup>10</sup>*Department of Medicine, Imperial College London, London, United Kingdom;*

<sup>11</sup>*Department of Nuclear Medicine and Tracer Kinetics, Osaka University, Japan;*

<sup>12</sup>*Nuclear Medicine Department, Royal Free Hospital, London, United Kingdom;*

<sup>13</sup>*Faculty of Biomedicine and Turku PET, Center, University of Turku, Turku, Finland*

<sup>14</sup>*Amallis Consulting LTD, London, United Kingdom;*

<sup>15</sup>*Medical Innovation, Value Evidence and Outcomes, GlaxoSmithKline R&D, Collegeville, Pennsylvania, USA;*

<sup>16</sup>*University Hospitals Coventry and Warwickshire, Coventry, United Kingdom;*

<sup>17</sup>*Derby Teaching Hospitals NHS Foundation Trust, Derby, United Kingdom;*

<sup>18</sup>*Department of Anesthesia, Critical Care and Pain Medicine, Massachusetts General Hospital and Harvard Medical School, Boston, Massachusetts, USA;*

<sup>19</sup>*Research and Early Development, Celgene, Cambridge, Massachusetts, USA; and*

<sup>20</sup>*Clinical Imaging, Clinical Pharmacology and Experimental Medicine, GlaxoSmithKline, Stevenage, United Kingdom*

*Current Word Count: 6482*

Corresponding Author:

Delphine L. Chen, MD

Professor of Radiology, University of Washington

Wil B. Nelp, MD Endowed Professorship in Nuclear Medicine

Director of Molecular Imaging, Seattle Cancer Care Alliance

1144 Eastlake Ave E # LG2-200

Seattle, WA 98109

Tel: 206-606-6777

Email: [dlchen7@uw.edu](mailto:dlchen7@uw.edu)

Running title: Lung FDG PET consensus recommendations

## NOTEWORTHY

- This consensus statement provides recommendations for  $^{18}\text{F}$ -fluorodeoxyglucose ( $^{18}\text{F}$ -FDG) PET lung imaging protocols, image analysis and reporting to facilitate the comparison of data acquired at different centers.
- Corrections for the effects of air (air fraction correction) and blood feature prominently in the quantitative analysis methods are proposed to improve lung tissue-specific  $^{18}\text{F}$ -FDG quantification.
- Minimizing respiratory motion effects on quantification remains challenging, which novel reconstruction methods and other approaches may help overcome.

## **ABSTRACT**

Positron emission tomography (PET) with  $^{18}\text{F}$ -fluorodeoxyglucose ( $^{18}\text{F}$ -FDG) has been increasingly applied, predominantly in the research setting, to study drug effects and pulmonary biology and monitor disease progression and treatment outcomes in lung diseases, disorders that interfere with gas exchange through alterations of the pulmonary parenchyma, airways and/or vasculature. To date, however, there are no widely accepted standard acquisition protocols and imaging data analysis methods for pulmonary  $^{18}\text{F}$ -FDG PET/CT in these diseases, resulting in disparate approaches. Hence, comparison of data across the literature is challenging. To help harmonize the acquisition and analysis and promote reproducibility, acquisition protocol and analysis method details were collated from seven PET centers. Based on this information and discussions among the authors, the consensus recommendations reported here on patient preparation, choice of dynamic versus static imaging, image reconstruction, and image analysis reporting were reached.

**Key words:** Pulmonary imaging, FDG, PET/CT, lung disease

## INTRODUCTION

Positron Emission Tomography (PET) has been explored in lung diseases, mostly in a research setting, as an imaging indicator of molecular changes for monitoring disease progression and treatment effects. The pathogenesis of these diseases leads to reduced gas exchange through alterations of the pulmonary parenchyma, airways and/or vasculature (1–4). However, the development of effective therapies remains disappointingly slow, hampered by the inability to quantify molecular changes in the lungs and assess drug binding and activity.  $^{18}\text{F}$ -Fluorodeoxyglucose ( $^{18}\text{F}$ -FDG) is the most widely available and commonly used PET tracer and is predominantly employed to assess lung inflammation and fibrosis-related processes for both research and clinical purposes. New molecularly-targeted PET tracers are also being developed to support the respiratory drug development process, with a recent publication demonstrating the additional potential for PET imaging to assess drug target engagement in the lungs (5). Therefore, we anticipate that the application of PET imaging in lung diseases will continue to grow across multiple centers.

In light of this growing use, standardization of acquisition protocols and analysis methods will facilitate data comparisons from multi-center studies and across the literature. To date, a range of analysis methods have been applied to disparately-acquired static and dynamic datasets in studies of lung disease and related processes (6–13). Given that the lungs uniquely contain varying amounts of air present depending on the disease, are the source of respiratory motion, and have relatively high fractional blood volume, special considerations are needed when applying quantitative imaging

approaches. Due to varying protocols among centers, however, comparability of the results across centers is somewhat limited.

Our group has previously published a summary of the conceptual approaches for lung PET imaging and highlighted some of the issues with clinical and research applications (2). To build on these applications and ensure comparability of data acquired across centers, we identified a need for harmonized protocols to enable cross-center data comparisons. Therefore, we convened representatives from all academic and commercial centers active in PET lung imaging to develop and present consensus recommendations for patient preparation, scanning protocol design, and imaging data analysis. The primary aim is to improve standardization to support uniform data collection and interpretation, thus improving the potential for result comparisons and data pooling across research studies and enable advancement of the field. Moreover, it is hoped that a better understanding of the origin of the PET signal, gained from studies using dynamic acquisition and complex analyses, will enable the development of simpler static measurement protocols that can be more readily applied in clinical practice. Our consensus recommendations are timely given the current higher level of attention on uniform protocols to enhance reproducibility of quantitative PET, as evidenced by recently published consensus papers in cancer and neuroimaging (14–17).

## **METHODS**

The acquisition protocols and image analysis details (Supplement Tables 1 and 2, Acquisition Protocols and Analysis Details) were collated from seven participating centers that have conducted PET studies in lung diseases (Cambridge University Hospitals NHS Foundation Trust & University of Cambridge; Invicro; Massachusetts General Hospital;

University College London; University Hospitals Coventry and Warwickshire; University of Edinburgh; and Washington University in St Louis, see Supplement Table 3). The acquisition protocol information included patient preparation, image acquisition, and image reconstruction. The analysis details included the whole and regional lung delineation methods and imaging endpoint derivations from both static and dynamic PET acquisitions. Between March 2018 and August 2019, the collated information was reviewed, and the consensus recommendations were developed over the course of three meetings, attended in person or via teleconference by representatives of the participating organizations. The acquisition protocol details collated were reviewed by all authors. Acquisition protocol differences among the centers were discussed and resolved to produce the consensus recommendations. When considering data analysis details, it was clear from the start that the desired imaging endpoints would vary among studies based on the specific study objectives. Therefore, the group defined minimum reporting requirements with a sufficient level of detail to enable published studies from different centers to be compared and to improve reproducibility of analysis. All authors reviewed and approved the recommendations in this paper.

## **RESULTS**

### **Patient Preparation**

*Fasting Period.* To minimize glucose-related inhibition of  $^{18}\text{F}$ -FDG uptake, only plain water should be consumed for a minimum six-hour fasting period prior to scanning. This is also the recommendation of the Quantitative Imaging Biomarkers Alliance for oncologic PET imaging (16).

*Blood Glucose Level.* Among the protocols collated, the minimum acceptable blood glucose level prior scanning varied. The authors agreed that a lower limit of 4 mmol/L would help avoid requiring glucose administration for preventing hypoglycemia that might interfere with the scan results. The European Association of Nuclear Medicine guidelines for tumor imaging (14) recommend an upper limit of 11 mmol/L for clinical studies. However, as medication such as steroids and other factors can influence glucose levels, the group felt this should be a guide, and upper limits should be determined on a per-study basis.

Similarly, regarding the fasting period and acceptable blood glucose and insulin levels for diabetic patients, there was insufficient data to make a firm recommendation. The group agreed that excluding patients with diabetes in small studies to minimize confounding factors was a reasonable consideration.

### **Patient Positioning and Comfort**

For pulmonary scanning, arm placement within the field of view (FOV) can cause computed tomography (CT) attenuation artifacts that may compromise the accuracy of the PET data. Therefore, having patients' arms above their head for the duration of the scan is preferred. For patients who cannot tolerate this position, ensuring that the arms fit completely within the CT FOV consistently is recommended to reduce inaccurate attenuation correction across the chest when comparing studies. A maximum body mass index of 35 kg/m<sup>2</sup> is generally suggested to minimize both variability in positioning of patients within the scanner and body habitus effects. The group also recommended that

patients with implants that are within the chest FOV, such as pacemakers, should be excluded from studies to avoid extreme artifacts.

Prolonged periods of lying down may be difficult for patients with lung diseases and may result in gross movement, causing attenuation correction errors. Measures should be taken to maximize comfort during scanning, including allowing continuous oxygen supply when needed; placing a vacuum bag filled with pillows or memory foam padding under the arms to provide support and improve blood circulation; and providing a variety of knee wedges for increasing back comfort and blankets for warmth (4). Appropriate padding of pressure points and avoidance of joint overstretching is particularly important for sedated, mechanically ventilated patients. Providing breaks during a dynamic PET scan for patients to sit or stand may be an option but will require rigorous realignment of each scan portion to produce a contiguous time-activity curve.

### **<sup>18</sup>F-FDG Administered Activities**

<sup>18</sup>F-FDG doses used for clinical oncologic scans as outlined in the European Association of Nuclear Medicine guidelines (14) are sufficient for a static clinical scan in most lung diseases. Since many factors determine the choice of injected activity, such as static or dynamic image acquisition, frame duration, desired analysis endpoints, and standard practice at the study location (see Supplement), no recommendation could be made to fit all studies. The advancement of more sensitive PET scanners could also affect the choice of injected dose. For research studies, the minimum activity that provides sufficient image quality to meet the study objectives should be used (18), and the group recommended that this should be determined on a per study basis.

*Injection Duration.* Very little published information is available regarding injection duration for dynamic acquisitions, even though this can influence the compartmental modelling (CM) results. Based on observations by several participating centers, a bolus with a shorter injection duration with adequate early-frame time sampling will better characterize the peak of the blood time-activity curve and may avoid a biased estimate of fractional blood volume ( $V_b$ , unitless), while a slow bolus injection may lead to improved fitting of the lung time-activity curves and a better estimate of the metabolic rate. Until these observations have been validated, a specific injection duration cannot be recommended. Until then, we recommend that the injection technique should be defined for each study protocol and reported accordingly, with steps taken to ensure consistency for all scans within a study, particularly where several personnel are involved.

## **IMAGE ACQUISITION**

### **Static Versus Dynamic Acquisitions**

Static PET imaging is the most common acquisition protocol used clinically. Static image endpoints have been shown to correlate with lung physiology and quality of life measurements (19) and thus may be sufficient to meet the study objectives. For example, static acquisitions may be sufficient for studies focused on areas of higher density, such as fibrotic regions or inflammatory nodules, that often demonstrate relatively high uptake levels. Using a reference region may also provide sufficient correction for differences in the blood signal due to systemic factors, such as variations in metabolism of the white blood cells within blood, without the need for a full kinetic model, as explored for idiopathic pulmonary fibrosis (12). Delayed post-injection static images may also help reduce the influence of blood activity by allowing blood activity to clear, as previously explored using

images obtained at 180 minutes post-injection (20). However, this may make quantification in normal lung tissue challenging due to the very low signal. Major advantages of static acquisitions include the short scanning duration that is well tolerated and broader accessibility as every clinical site will have the capacity to acquire and analyze the data.

Dynamic imaging enables kinetic parameter estimation and can provide additional insights into the origins of the PET signal. Kinetic modelling of blood and lung cell compartments (parenchymal, airway wall, vascular wall and immune cells (2)) to enable corrections for  $V_b$  contributions may be achievable (11,21), thus making dynamic acquisitions an important consideration when attempting to account for such effects with a single tracer. Additionally, dynamic scan parameters have been shown to be more sensitive in quantifying the presence of low-level lung inflammation when compared to static endpoints in certain conditions, such as in acute lung injury models (22), and in discriminating the sources of increased FDG uptake in different mechanisms of injury (23). The aims of each research study will define the optimal approach, and the choice should be justified when the study is reported.

The effect of the partial volume of air in each voxel will affect both static and dynamic acquisitions and may vary between different lung regions. This can be corrected by using appropriately acquired CT images matched to the PET images for respiration, referred to as “air fraction correction” hereafter. As new tracers are introduced for lung imaging, the kinetics and dynamic range of uptake will also be important factors in deciding between static and dynamic acquisitions.

## Accounting for Respiratory Motion

Due to the unique function of the lungs, the large variation in air volume with normal respiration can reduce PET quantitation accuracy. Clinical CT examinations are routinely performed at breath-hold, often at full inspiration. Since respiration must occur during the longer durations of static and dynamic PET scans, locally varying displacement and compression of tissues will potentially contribute to errors in both attenuation correction and air fraction correction. The displacement causes blurring and increases the partial volume effect, particularly near the diaphragm, whereas the compression of tissues affects density and radiotracer concentration (24). Mismatch between the point in the respiratory cycle at which the CT scan used for attenuation correction is acquired and the average position represented by the PET data can therefore lead to attenuation correction as well as air fraction correction artifacts and is an important source of error.

Multiple approaches to remove or limit respiratory motion have been investigated. Shallow breathing during the CT acquisition or breath-holds at gentle end-expiration, as for cancer imaging (e.g. (25)) or at mid-expiration for idiopathic pulmonary fibrosis patients (26,27) can minimize the effects of misregistration of PET and CT images due to respiratory motion. Visual feedback systems have been used to monitor and display the lung volume continuously to the subject but are not widely adopted (28). The use of a repeated breath-hold acquisition has also been suggested (29) but can be difficult for those with reduced lung function. Longer duration CT scans acquired over the respiratory cycle, such as CINE-CT or low-pitch helical CT, can be used to create averaged CT scans (e.g. (30)). A four-dimensional CT dataset sorted according to the respiratory signal can be used with gated PET data (31), with several studies investigating various respiratory

gating strategies for PET (e.g. (32)). Interpolated averaged CT scans constructed from full inspiration and end-expiration scans may also be considered (33), a method that could also be applied to CT scans obtained from dynamic imaging protocols in which breaks are built into the dynamic acquisition (34).

The approach most used amongst the centers to minimize PET and CT misregistration was breath-hold at gentle end-expiration or at mid-expiration for the CT scan. Pre-scan coaching to familiarize the patient with breathing instructions improved compliance and is thus recommended. Since many of the advanced techniques described above are not widely available and require post-imaging offline processing, we recommend that, for research studies, list-mode acquisitions be acquired and stored for future reprocessing when respiratory gating and other advanced techniques to minimize respiratory motion become readily available.

### **Acquisition Duration and Time-Frame for Dynamic Acquisitions**

Clinical static  $^{18}\text{F}$ -FDG PET imaging protocols have been used successfully to image lung disease (19). Typically, data are acquired over a short interval starting approximately 60 minutes after tracer injection. For dynamic imaging studies, acquisitions start at the same time as tracer administration and range from 45 to 90 minutes in duration. The scan durations reported by the centers are routinely tolerated without discomfort or safety issues and allow robust kinetic analysis. Typically, short frames are used initially to capture the early dynamics of the tracer in blood followed by frames of longer duration later in the acquisition. For a typical 60-minute scan, our recommended time-frames are: 5-15 sec/frame for the first 2 min post injection; 20-30 from 2-5 mins; 60 from 5-10 mins;

120 for 10-18 mins; 180 for 18-30 mins; and 300 for 30-60 mins post injection. We again recommend retaining the list-mode data to allow future exploration of different time-frames.

Most modern PET/CT scanners can cover the entire lung at gentle end-expiration in a single bed position. For those requiring two bed positions to cover the entire lung, a dynamic data acquisition initially over one bed position followed by a static data acquisition with two bed positions to cover the whole lung may be used. Alternating two bed positions over the scan duration, such as alternating seven 4-minute acquisitions for each position, is another approach that more easily accommodates breaks between the bed position scans. Breaks should be scheduled to avoid disrupting the acquisition of the time-activity curve peak during the vascular phase post-injection (see Figure 1). The recently developed total body PET scanner (35) will eliminate the need for such protocols but is not widely available.

## **IMAGE RECONSTRUCTION**

Various PET image reconstruction algorithms are available with different algorithms leading to different noise and image characteristics, depending on the choice of parameters, filters or *a priori* assumptions (36). Further, for iterative algorithms, the convergence rate of the values in low-count regions such as the lungs is often lower than in high-count regions (37,38). This may affect the observed radiotracer concentration in the lung; therefore, we recommend using a large number of iterative updates (i.e., number of iterations times number of subsets) to ensure uniform convergence (38,39). The group agreed that more investigation was needed to define optimal reconstruction specifically for lung PET imaging and therefore could not make specific recommendations based on

current data. Additionally, the development of specific phantoms that model relevant aspects of lung physiology and support the establishment of harmonization standards will be needed to support multicenter studies.

Time-of-flight (TOF) PET scanners have been shown to reduce noise, especially in large patients (40). In addition, the local effects of attenuation mismatch between reconstructed PET and CT images of non-TOF PET are reduced (41–43), albeit at the expense of non-local effects outside the lung (27). Although TOF PET/CT scanners have become more widely available, insufficient data are available to make a firm recommendation on whether TOF is valuable for quantitative lung imaging. For multicenter studies, we recommend that either data from scanners with a similar TOF time resolution are used (44) or that only non-TOF reconstructed images are used for consistent results.

Table 1 summarizes recommendations on patient preparation, acquisition protocol and image reconstruction.

## **IMAGE ANALYSIS REPORTING**

Quantitative PET pulmonary image analysis involves extracting volumes of interest (VOIs) and quantifying the  $^{18}\text{F}$ -FDG signal within the VOIs. As different study requirements preclude an absolute recommendation of a single methodology for all future studies, it was agreed that consistent reporting, in accordance with the guidelines below, would enable better comparison of studies and interpretation of findings from future studies.

## **Whole Lung Analysis**

Use of the attenuation correction CT for lung segmentation is recommended. For consistency, performing a quality control check on the segmented lung mask is essential to exclude the chest wall, major airways, bullae, heart, and liver. The lung mask created in CT space should be resampled to PET resolution, for which we recommend using the nearest neighbor method to obtain a binary mask suitable for VOI processing. In the presence of any gross movement of the patient during the PET and CT acquisitions, the images should be registered to minimize the differences. Details should be provided on methods for lung mask segmentation PET and CT alignment confirmation.

## **Regional Lung Analysis**

To investigate regional  $^{18}\text{F}$ -FDG distribution, the whole lung mask can be subdivided into multiple regions by either anatomical lobes, such as through fissure detection (45), or simple geometric division into upper, middle, and lower lung zones based on either length or volume (10,11). Similarly, anterior-posterior sub-divisions and regions with different densities have also been used. There is insufficient information to recommend a single optimal approach and this may also vary with disease. Therefore, we recommend reporting all regional analysis details, including definition and selection of VOI location and size.

## Quantification of $^{18}\text{F}$ -FDG uptake

Static and dynamic analysis techniques have been investigated to account for various lung-specific issues in PET quantification as described above. Below we describe the consensus recommendations for reporting these quantities.

*Static Data Analysis.* The maximum standard uptake value ( $SUV_{max}$ , unitless), defined as the highest single voxel value within a VOI, is the most widely used measure of  $^{18}\text{F}$ -FDG uptake and warrants investigation despite several potential confounding factors that could influence its measurement, including partial volume averaging effects (15). Corrections to the SUV for fractional air volume ( $V_a$ , unitless) and  $V_b$ , when independently measured, should be applied and reported (46,47). The peak SUV, without or with correction for lean body mass ( $SUL_{peak}$ , unitless), measured from an approximately  $1\text{ cm}^3$  VOI the highest value as defined for PET Response Criteria for Imaging Tumors (48), is less influenced by image noise and may also be considered. Comparing areas of diseased to normal lung to determine a target-to-background ratio (unitless) as well as characterizing lung heterogeneity may also be useful approaches (12,49).

*Dynamic Data Analysis.* Dynamic datasets can be analyzed using either Patlak Graphical Analysis (PGA) or CM. In both cases, an input function is required to describe the time-course of radioactivity concentration in arterial plasma. An image-derived input function (IDIF) may be obtained from the dynamic PET in preference to blood sampling. IDIFs from the pulmonary artery, ascending aorta, descending aorta, and superior vena cava have been investigated (50). In the combined experience among the authors, the

use of pulmonary artery, ascending aorta, and descending aorta reached similar outcomes for rate of transfer of  $^{18}\text{F}$ -FDG,  $K_i$  ( $\text{mL}_{\text{plasma}}/\text{mL}_{\text{lung}}/\text{min}$ ) (51,52). The right ventricle can also be used as an IDIF source (53) but is not useful if this is not consistently included in the FOV for lung PET scans. Time delays between passage of the tracer through the IDIF VOI and the tissue of interest may affect blood volume estimates but is less important for the influx constant  $K_i$  (see next section). The size of VOI should be reported and should be consistent for all patients within the same study.

*Patlak Graphical Analysis:* PGA estimates the net influx rate of irreversibly trapped tracers such as  $^{18}\text{F}$ -FDG from the blood into target tissue ( $K_i$ ) and an approximate steady-state partition coefficient between tissue and plasma of non-phosphorylated  $^{18}\text{F}$ -FDG ( $V_{ss}$ ,  $\text{mL}/\text{cm}^3$ ) (54).  $V_{ss}$  was initially assumed to reflect changes in density, leading to explorations of normalizing  $K_i$  with  $V_{ss}$  (6). However, normalizing the  $K_i$  by the Patlak intercept has been shown algebraically to remain sensitive to changes in  $V_a$  and  $V_b$  (11,21). Therefore, caution is advised in its application and interpretation as a measure of the true net influx rate. For accurate comparison, the results of PGA should include both  $K_i$  and  $V_{ss}$  individually if normalized  $K_i$  is used, as reported previously (6,10–12).

*Compartmental Modelling:* Non-linear regression models are used to estimate the microparameters of the model ( $K_1$  ( $\text{mL}_{\text{plasma}}/\text{mL}_{\text{lung}}/\text{min}$ ),  $k_2$  (1/min),  $k_3$  (1/min)) and the blood contribution ( $V_b$ ) from lung time-activity curves and the IDIF, to then estimated  $K_i$  using a two-compartment model (2). Since  $^{18}\text{F}$ -FDG can be considered irreversibly trapped over the timeframe for the scan,  $k_4$  is assumed to be zero. Air fraction correction

may also be included in the CM, for which net influx rate is denoted as  $K_{ic}$  (11,50). The quality of the fit of the data should be assessed and reported using a metric such as chi-squared. Care should be taken to report the CM method accurately to enable reproducibility given various approaches available. The presence of edema in some conditions such as acute lung injury may require an additional compartment (55).

Table 2 summarizes image analysis parameter reporting. Table 3 lists CM-specific parameters that the group recommends for reporting to promote reproducibility (56).

## **CONCLUSION**

To improve both reproducibility and potential for data pooling between centers and reproducibility for studies within a given center, investigators using PET/CT in studies of lung disease are urged to follow the recommendations presented in this manuscript when designing, conducting and reporting studies. As highlighted above, ample opportunities for investigation exist to improve the methods used to acquire and analyze lung PET/CT images. We hope this summary will serve as a basis from which we can advance the field of lung PET imaging.

## **ACKNOWLEDGEMENTS**

The authors acknowledge the late Martin Connell for his tremendous contributions to the PET in Lung Diseases Collaboration Initiative and his dedication to the field of quantitative medical imaging analysis. The Institute of Nuclear Medicine at UCL receives support from the NIHR University College London Hospitals Biomedical Research Centre. The National Physical Laboratory is supported by funding from the National Measurement System program of the UK's Department of Business, Energy and Industrial Strategy. JC

acknowledges funding support from the Cambridge NIHR Comprehensive Biomedical Research Centre and GlaxoSmithKline. EvB is supported by the Scottish Imaging Network (SINAPSE). LV acknowledges funding support from EPSRC.

## **FINANCIAL DISCLOSURES**

DLC: Funding from National Institutes of Health (R01 HL121218, R01 HL131908, P41 EB025815). LC: Pfizer, Inc, employee and shareholder. JC: obligation to spend 50% of NHS time for GlaxoSmithKline. BFH, KT, KE: GlaxoSmithKline, GE Healthcare, Siemens Healthineers and Kromek funding. AR, EE: GlaxoSmithKline funding. SL: Amallis employee and company director; GE Healthcare and GlaxoSmithKline consulting fees. DM, RT-S: GlaxoSmithKline former employee. DM: Genentech/Roche current employee and shareholder. FJW: GlaxoSmithKline employee and shareholder. RT-S: GlaxoSmithKline shareholder; Immunomet, Vocalis Health and Ena Therapeutics consulting fees. GR: Employee of inviCRO. EvB: owner, QCTIS Ltd, Aidence and Imbio advisory boards, funding from Siemens, GE Healthcare, and Alliance Medical. MFVM: funding from NIH-NHLBI RO1 HL121228. LV: GSK funding (STU100043346, BIDS3000023795); JWW: Celgene employee and shareholder. No other potential conflicts of interest relevant to this article exist.

## REFERENCES

1. Scherer P, Chen D. Imaging Pulmonary Inflammation. *J Nucl Med*. 2016;57:1764-1770.
2. Chen DL, Cheriyan J, Chilvers ER, et al. Quantification of lung PET Images: challenges and opportunities. *J Nucl Med*. 2017;58:201-207.
3. Lukey PT, Harrison SA, Yang S, et al. A randomised, placebo-controlled study of omipalisib (PI3K/mTOR) in idiopathic pulmonary fibrosis. *Eur Respir J*. 2019;53:1801992.
4. Chen DL, Huang HJ, Byers DE, et al. The peroxisome proliferator-activated receptor agonist pioglitazone and 5-lipoxygenase inhibitor zileuton have no effect on lung inflammation in healthy volunteers by positron emission tomography in a single-blind placebo-controlled cohort study. *PLOS ONE*. 2018;13:e0191783.
5. Maher TM, Simpson JK, Porter JC, et al. A positron emission tomography imaging study to confirm target engagement in the lungs of patients with idiopathic pulmonary fibrosis following a single dose of a novel inhaled  $\alpha\beta6$  integrin inhibitor. *Respir Res*. 2020;21:75.
6. Jones HA, Sriskandan S, Peters AM, et al. Dissociation of neutrophil emigration and metabolic activity in lobar pneumonia and bronchiectasis. *Eur Respir J*. 2003;10:795-803.
7. Chen DL, Rosenbluth DB, Mintun MA, Schuster DP. FDG-PET imaging of pulmonary inflammation in healthy volunteers after airway instillation of endotoxin. *J Appl Physiol*. 2006;100:1602-1609.
8. Chen DL, Bedient TJ, Kozlowski J, et al. [18F]Fluorodeoxyglucose positron emission tomography for lung antiinflammatory response evaluation. *Am J Respir Crit Care Med*. 2009;180:533-539.
9. Harris RS, Venegas JG, Wongviriyawong C, et al. 18F-FDG Uptake Rate Is a Biomarker of Eosinophilic Inflammation and Airway Response in Asthma. *J Nucl Med*. 2011;52:1713-1720.
10. Subramanian D, Jenkins L, Edgar R, Quraishi N, Stockely R, Parr D. Assessment of pulmonary neutrophilic inflammation in emphysema by quantitative positron emission tomography. *Am J Respir Crit Care Med*. 2012;186:1125-1132.
11. Coello C, Fisk M, Mohan D, et al. Quantitative analysis of dynamic 18F-FDG PET/CT for measurement of lung inflammation. *EJNMMI Res*. 2017;7:47.
12. Win T, Screatton NJ, Porter JC, et al. Pulmonary 18F-FDG uptake helps refine current risk stratification in idiopathic pulmonary fibrosis (IPF). *Eur J Nucl Med Mol Imaging*. 2018;45:806-815.

13. Motta-Ribeiro GC, Hashimoto S, Winkler T, et al. Deterioration of regional lung strain and inflammation during early lung injury. *Am J Respir Crit Care Med*. 2018;198:891-902.
14. Boellaard R, Delgado-Bolton R, Oyen WJG, et al. FDG PET/CT: EANM procedure guidelines for tumour imaging: version 2.0. *Eur J Nucl Med Mol Imaging*. 2015;42:328-354.
15. Kinahan PE, Perlman ES, Sunderland JJ, et al. The QIBA Profile for FDG PET/CT as an imaging biomarker measuring response to cancer therapy. *Radiology*. 2020;294:647-657.
16. FDG-PET/CT Technical Committee. QIBA profile. FDG-PET/CT as an imaging biomarker measuring response to cancer therapy. November 2016.
17. Knudsen GM, Ganz M, Appelhoff S, et al. Guidelines for the content and format of PET brain data in publications and archives: a consensus paper. *J Cereb Blood Flow Metab*. 2020;40:1576-1585.
18. International commission on radiological protection. Radiological protection in biomedical research. *ICRP Publ 62 Annu ICRP*. 1992;22.
19. Groves AM, Win T, Screatton NJ, et al. Idiopathic pulmonary fibrosis and diffuse parenchymal lung disease: implications from initial experience with 18F-FDG PET/CT. *J Nucl Med*. 2009;50:538-545.
20. Umeda Y, Demura Y, Morikawa M, et al. Prognostic Value of Dual-Time-Point 18F-FDG PET for Idiopathic Pulmonary Fibrosis. *J Nucl Med*. 2015;56:1869-1875.
21. Holman BF, Cuplov V, Millner L, et al. Improved correction for the tissue fraction effect in lung PET/CT imaging. *Phys Med Biol*. 2015;60:7387-7402.
22. Chen DL, Mintun MA, Schuster DP. Comparison of methods to quantitate 18F-FDG uptake with PET during experimental acute lung injury. *J Nucl Med*. 2004;45:1583-1590.
23. de Prost N, Feng Y, Wellman T, et al. 18F-FDG kinetics parameters depend on the mechanism of injury in early experimental acute respiratory distress syndrome. *J Nucl Med*. 2014;55:1871-1877.
24. Cuplov V, Holman B, McClelland J, Modat M, Hutton B, Thielemans K. Issues in quantification of registered respiratory gated PET/CT in the lung. *Phys Med Biol*. 2017;63:015007.
25. Gilman MD, Fischman AJ, Krishnasetty V, Halpern EF, Aquino SL. Optimal CT breathing protocol for combined thoracic PET/CT. *Am J Roentgenol*. 2006;187:1357-1360.

26. Holman B, Cuplov V, Hutton B, Groves A, Thielemans K. The effect of respiratory induced density variations on non-TOF PET quantitation in the lung. *Phys Med Biol*. 2016;61:3148-3163.
27. Emond EC, Bousse A, Machado M, et al. Effect of attenuation mismatches in time of flight PET reconstruction. *Phys Med Biol*. 2020;65:085009.
28. Harris RS, Winkler T, Musch G, et al. The prone position results in smaller ventilation defects during bronchoconstriction in asthma. *J Appl Physiol*. 2009;107:266-274.
29. Skretting A, Revheim M, Knudtsen I, Johnsrud K, Bogsrud T. An implementation of time-efficient respiratory-gated PET acquisition by repeated breath-holds. *Acta Radiol*. 2013;54:672-675.
30. Pan T, Mawlawi O, Luo D, et al. Attenuation correction of PET cardiac data with low-dose average CT in PET/CT. *Med Phys*. 2006;33:3931-3938.
31. Moorees J, Bezak E. Four dimensional CT imaging: a review of current technologies and modalities. *Australas Phys Eng Sci Med*. 2012;35:9-23.
32. Bettinardi V, De Bernardi E, Presotto L, Gilardi M. Motion-tracking hardware and advanced applications in PET and PET/CT. *PET Clin*. 2013;8:11-28.
33. Mok GSP, Tao Sun, Tzung-Chi Huang, Vai MI. Interpolated average CT for attenuation correction in PET—a simulation study. *IEEE Trans Biomed Eng*. 2013;60:1927-1934.
34. Holman BF, Cuplov V, Millner L, et al. Improved quantitation and reproducibility in multi-PET/CT lung studies by combining CT information. *EJNMMI Phys*. 2018;5:14.
35. Cherry SR, Jones T, Karp JS, Qi J, Moses WW, Badawi RD. Total-Body PET: maximizing sensitivity to create new opportunities for clinical research and patient care. *J Nucl Med*. 2018;59:3-12.
36. Defrise M, Kinahan PE, Michel CJ. Image reconstruction algorithms in PET. In: Bailey DL, Townsend DW, Valk PE, Maisey MN, eds. *Positron Emission Tomography*. London: Springer-Verlag; 2005:63-91.
37. Hutton BF, Hudson HM, Beekman FJ. A clinical perspective of accelerated statistical reconstruction. *Eur J Nucl Med*. 1997;24:797-808.
38. Boellaard R, van Lingen A, Lammertsma A. Experimental and clinical evaluation of iterative reconstruction (OSEM) in dynamic PET: quantitative characteristics and effects on kinetic modeling. *J Nucl Med*. 2001;42:808-17.

39. Jaskowiak CJ, Bianco JA, Perlman SB, Fine JP. Influence of reconstruction iterations on 18F-FDG PET/CT standardized uptake values. *J Nucl Med*. 2005;46:424-428.
40. Watson CC. An evaluation of image noise variance for time-of-flight PET. *IEEE Trans Nucl Sci*. 2007;54:1639-1647.
41. Turkington TG, Wilson JM. Attenuation artifacts and time-of-flight PET. In: 2009 IEEE Nuclear Science Symposium Conference Record (NSS/MIC). Orlando, FL, USA: IEEE; 2009:2997-2999.
42. Ahn S, Cheng L, Manjeshwar RM. Analysis of the effects of errors in attenuation maps on PET quantitation in TOF PET. In: 2014 IEEE Nuclear Science Symposium and Medical Imaging Conference (NSS/MIC). Seattle, WA, USA: IEEE; 2014:1-4.
43. Thielemans K, Asma E, Manjeshwar RM, Ganin A, Spinks TJ. Image-based correction for mismatched attenuation in PET images. In: 2008 IEEE Nuclear Science Symposium Conference. Dresden, Germany: IEEE; 2008:5292-5296.
44. Kotasidis FA, Mehranian A, Zaidi H. Impact of time-of-flight on indirect 3D and direct 4D parametric image reconstruction in the presence of inconsistent dynamic PET data. *Phys Med Biol*. 2016;61:3443-3471.
45. Pu J, Zheng B, Leader JK, et al. Pulmonary lobe segmentation in CT examinations using implicit surface fitting. *IEEE Trans Med Imaging*. 2009;28:1986-1996.
46. Lambrou T, Groves AM, Erlandsson K, et al. The importance of correction for tissue fraction effects in lung PET: preliminary findings. *Eur J Nucl Med Mol Imaging*. 2011;38:2238-2246.
47. Valind SO, Rhodes CG, Brudin LH, Jones T. Measurements of regional ventilation pulmonary gas volume: theory and error analysis with special reference to positron emission tomography. *J Nucl Med*. 1991;32:1937-1944.
48. Wahl RL, Jacene H, Kasamon Y, Lodge MA. From RECIST to PERCIST: evolving considerations for PET response criteria in solid tumors. *J Nucl Med*. 2009;50:122S-150S.
49. Winkler T, Vidal Melo MF, Degani-Costa LH, et al. Estimation of noise-free variance to measure heterogeneity. *PLOS ONE*. 2015;10:e0123417.
50. Holman BF. Improving quantification of PET/CT biomarkers for evaluation of disease progression and treatment effectiveness in pulmonary fibrosis. 2016.
51. van der Weerd AP, Klein LJ, Boellaard R, Visser CA, Visser FC, Lammertsma AA. Image-derived input functions for determination of MRGlu in cardiac 18F-FDG PET scans. *J Nucl Med*. 2001;42:1622-1629.

52. de Geus-Oei L-F, Visser EP, Krabbe PFM, et al. Comparison of image-derived and arterial input functions for estimating the rate of glucose metabolism in therapy-monitoring 18F-FDG PET studies. *J Nucl Med*. 2006;47:945-949.
53. Schuster D, Kaplan J, Gauvain K, Welch M, Markham J. Measurement of regional pulmonary blood flow with PET. *J Nucl Med*. 1995;36:371-7.
54. Patlak CS, Blasberg RG, Fenstermacher JD. Graphical evaluation of blood-to-brain transfer constants from multiple-time uptake data. *J Cereb Blood Flow Metab*. 1983;3:1-7.
55. Schroeder T, Vidal Melo MF, Musch G, Harris RS, Venegas JG, Winkler T. Modeling pulmonary kinetics of 2-deoxy-2-[18F]fluoro-D-glucose during acute lung injury. *Acad Radiol*. 2008;15:763-775.
56. Vass LD, Lee S, Wilson FJ, Fisk M, Cheriyan J, Wilkinson I. Reproducibility of compartmental modelling of 18F-FDG PET/CT to evaluate lung inflammation. *EJNMMI Phys*. 2019;6:26.

**Table 1.** Recommendations on Patient Preparation, Acquisition Protocol, and Image Reconstruction.

| <b>CATEGORY</b>   | <b>RECOMMENDATION</b>   |
|---|---|
| <b>Patient Preparation</b>                                |   |
| <b>Fasting Period</b>                                     | Use minimum 6 hours prior to scanning with plain water allowed.   |
| <b>Blood Glucose Level</b>                                | Allow minimum 4 mmol/L.<br><br>Determine upper limit by study objectives.   |
| <b>Patient Positioning</b>                                | Position arms above head whenever possible.<br><br>Allow maximum BMI of 35 kg/m <sup>2</sup> for consistent arm positioning.  |
| <b>FDG Administered Activities and Injection Duration</b> | Use minimum activity needed for sufficient image quality to meet study objectives.<br><br>Document injection duration and use consistently for all patients in the study.   |
| <b>Acquisition Protocol</b>                               |   |
| <b>Static versus Dynamic Acquisitions</b>                 | Use of static scans acceptable if compatible with the study objectives.<br><br>Recommend dynamic scans when tracer quantification for specific lung compartments needed.<br><br>Report rationale for the chosen acquisition method per study.   |
| <b>Respiratory Gating</b>                                 | Report end-expiration gating results when used.   |
| <b>Accounting for Respiratory Motion</b>                  | Store list-mode data to allow future reprocessing as techniques improve.<br>Breath-hold at end-expiration or mid-expiration most frequently used to match lung volumes for CT and PET.<br><br>Pre-scan coaching of breathing instructions recommended.<br><br>Coaching the patient on breathing instructions for the attenuation correction CT can minimize most respiratory motion errors.<br><br>Approaches such as cine-CT should be explored.   |
| <b>Acquisition duration and time-frames</b>               | Static imaging: starting at 60 minutes post injection (p.i.)<br><br>Dynamic imaging: 45-90 minute acquisition starting immediately p.i.; a 60-minute scan is routinely tolerated (breaks may be required for improved patient tolerance).<br><br>Time-frames for a typical 60-minute dynamic acquisition (time p.i. in minutes): 0-2 mins: 5-15 sec/frame; 2-5 mins: 20-30 sec/frame; 5-10 mins: 60 sec/frame; 10-18 mins: 120 sec/frame; 18-30 mins: 180 sec/frame; and 30-60 mins: 300 sec/frame. |
| <b>Image Reconstruction</b>                               | Method should be harmonized as much as possible in a multi-center study.<br><br>When using iterative reconstruction, a larger number of iterations should be considered to ensure uniform convergence, regardless of the specific image reconstruction algorithm, followed by a suitable filter to control noise if desired.  |

**Table 2.** Recommendations on image analysis parameters.

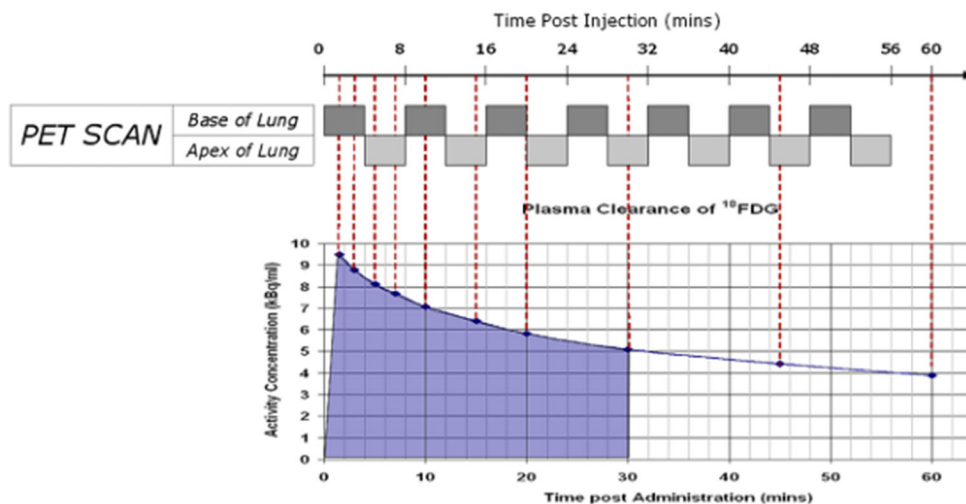
| <b>IMAGING MODALITY</b> | <b>ANALYSIS METHODS</b>                   | <b>ABBREVIATION</b> | <b>EXPLANATION</b>   |
|-------------------------|---|---------------------|--|
| <b>Static</b>           | Maximum body-weight standard uptake value | $SUV_{max}$         | Maximum standard uptake value* (unitless)  |
| <b>Dynamic</b>          | Patlak                                    | $K_i$               | Net influx rate of $^{18}\text{F}$ -FDG* (mL <sub>plasma</sub> /mL <sub>lung</sub> /min)                                   |
|                         |   | $V_{ss}$            | Steady-state partition coefficient (ml/cm <sup>3</sup> )   |
|                         | Compartmental Modelling                   | $K_{ic}$            | Net influx rate of $^{18}\text{F}$ -FDG (mL <sub>plasma</sub> /mL <sub>lung</sub> /min) (from $K_1$ , $k_2$ , and $k_3$ )* |
|                         |   | $V_b$               | Fractional blood volume (unitless)   |
| <b>CT</b>               | Air fraction determination                | $V_a$               | Fractional air volume (unitless)   |

\*Air fraction correction may be applied using  $V_a$

**Table 3.** Recommendations on minimum compartmental modelling method parameters to be reported

| <b>METHOD<br/>PARAMETER</b>          | <b>EXPLANATION</b>                                       |
|--------------------------------------|--|
| <b>Weighting Factors</b>             | How factors were calculated                              |
| <b>Time Delay</b>                    | Method used to fit the time delay                        |
| <b>Input Function<br/>Modelling</b>  | Method used to define input function                     |
| <b>Vessel Volume</b>                 | Size, position, and methods used for vessel segmentation |
| <b>Lung volumes-of-<br/>interest</b> | Method used for whole/regional lung segmentation         |
| <b>Goodness of fit</b>               | Method used for evaluating data fitting                  |

Figure 1 Illustration of alternating two bed positions over the scan duration. A 4-minute acquisition phase for each bed position enabled data collection from the lung apex and base. Blood sampling times are indicated by the dashed red lines and blood activity is shown by the blue line. (Reprinted with permission of (10))





The Journal of  
NUCLEAR MEDICINE

## Consensus recommendations on the use of $^{18}\text{F}$ -FDG PET/CT in lung disease

Delphine L. Chen, Safia Ballout, Laigao Chen, Joseph Cheriyan, Gourab Choudhury, Ana M. Denis-Bacelar, Elise Emond, Kjell Erlandsson, Marie Fisk, Francesco Fraioli, Ashley M. Groves, Roger N. Gunn, Jun Hatazawa, Beverly F. Holeman, Brian F. Hutton, Hidehiro Iida, Sarah Lee, William MacNee, Keiko Matsunaga, Divya Mohan, David Parr, Alelah Rashidnasab, Gaia Rizzo, Deepak Subramanian, Ruth Tal-Singer, Kris Thielemans, Nicola Tregay, Edwin J.R. Van Beek, Laurence Vass, Marcos F. Vidal Melo, Jeremy W. Wellen, Ian Wilkinson, Frederick J. Wilson and Tilo Winkler

*J Nucl Med.*

Published online: September 18, 2020.

Doi: 10.2967/jnumed.120.244780

---

This article and updated information are available at:

<http://jnm.snmjournals.org/content/early/2020/09/18/jnumed.120.244780>

---

Information about reproducing figures, tables, or other portions of this article can be found online at:

<http://jnm.snmjournals.org/site/misc/permission.xhtml>

Information about subscriptions to JNM can be found at:

<http://jnm.snmjournals.org/site/subscriptions/online.xhtml>

---

*JNM* ahead of print articles have been peer reviewed and accepted for publication in *JNM*. They have not been copyedited, nor have they appeared in a print or online issue of the journal. Once the accepted manuscripts appear in the *JNM* ahead of print area, they will be prepared for print and online publication, which includes copyediting, typesetting, proofreading, and author review. This process may lead to differences between the accepted version of the manuscript and the final, published version.

---

*The Journal of Nuclear Medicine* is published monthly.  
SNMMI | Society of Nuclear Medicine and Molecular Imaging  
1850 Samuel Morse Drive, Reston, VA 20190.  
(Print ISSN: 0161-5505, Online ISSN: 2159-662X)

© Copyright 2020 SNMMI; all rights reserved.